PHYSICAL REVIEW B VOLUME 24, NUMBER 10 15 NOVEMBER 1981

Theoretical study of the electronic structure of SiO_x

E. Martinez and Felix Ynduráin
Departamento de Física Fundamental, Universidad Autónoma de Madrid, Canto Blanco, Madrid 34, Spain
(Received 9 April 1981)

A theoretical study of the electronic structure of amorphous SiO_x is performed. The calculation is done using a realistic tight-binding Hamiltonian for a cluster-Bethe-lattice model. Results of the calculations are in good agreement with optical-absorption measurements for the entire range of concentrations and with photoemission spectra for $x = 0$, 1, and 2. The nonlinear variation of the optical gap with concentration that takes place at $x = 1.5$ is related to the break of Si chains and to the percolation threshold. Comparison with photoemission data shows that the Si–O–Si bond angle is $\sim 125°$ in agreement with chemical shift analysis. Our study indicates that the distribution is Si and O atoms in a-SiO_x is random with no O–O bonds. It is found that intermediate range order plays a fundamental role in the electronic structure of a-SiO_x.

I. INTRODUCTION

The oxidation of Si to form a Si-SiO_2 interface is an open problem in solid-state physics.[1] The electronic structure of both the Si surface and bulk SiO_2 are well understood, but the only well-established feature of the Si-SiO_2 interface is that oxygen saturates the Si surface dangling bonds. Whether the removal of states from the Si gap is complete or not is still controversial.

From the experimental point of view it seems that there is evidence for the existence of an intermediate transition region at the Si-SiO_2 interface. The width and stoichiometry of this region is not well established. We can then visualize the Si-SiO_2 system as being formed by Si-SiO_x-SiO_2, where the interface alloy SiO_x is to be characterized. The local atomic structure at the Si-SiO_2 interface has been investigated using high-resolution x-ray photoelectron spectroscopy by Grunthaner *et al.*[2] This study is based on the variation of the chemical shift with the bridging Si–O–Si bond angle. A simple interpolation scheme based on a tight-binding calculation indicates that the Si–O–Si bond angle at the interface is mostly 125° instead of being 144° as in bulk SiO_2. This estimated bond angle allows the characterization of the ring statistics at the interface.

Hollinger, using ultraviolet photoemission (UPS) techniques, has been able to conclude that the electronic structure of SiO_x for $x=1$ and the Si-SiO_2 interface are very similar.[3] We then think that it is worthwhile studying the electronic structure of SiO_x itself before making a detailed study of the Si-SiO_2 interface. The available experimental information on SiO_x reveals important differences with respect to SiO_2 and Si. UPS experiments[4] on SiO show that its spectrum cannot be reproduced by taking the average of the Si and SiO_2 spectra. Optical-absorption measurements of SiO_x for the entire range of concentrations[5,6] indicate a nonsmooth variation of the optical gap with the concentration showing an abrupt change of the gap at about $x=1.5$. Also, an analysis of the form of the optical-absorption curves near threshold indicate a change in the localization of the states at the top of the valence band near $x=1.5$. A detailed study of these experiments can contribute to the understanding of both the Si–O bond and the atomic structure of the alloy.

In this work we have developed a model aimed at describing the electronic structure of SiO_x. A theory of the electronic structure of SiO_x has to answer the following points: (i) Which is the local bonding in the SiO_x alloy? (ii) Which is the atomic structure of the alloy and, in particular, which is the bond angle Si–O–Si? (iii) Which are the bonding statistics so that we can distinguish between the random-bonding model and the mixture model?[5,7] (iv) Why does the optical absorption have a very nonlinear variation with concentration and why does the slope of the absorption coefficient vary with x?

This work is organized as follows. In Sec. II we made an extension of the cluster-Bethe-lattice method to study alloys where the chemical bonding is different at the two extreme concentrations. The tight-binding Hamiltonian used in this work is also discussed in this section. The electronic density of states of the SiO_x alloy for different concentrations is presented. In Sec. III a detailed comparison with the available experimental data is made. Based on this comparison we discuss the bonding statistics in the alloy and its atomic structure. In Sec. IV the conclusions of our work are summarized.

II. STUDY OF THE ELECTRONIC STRUCTURE OF SiO_x

Before we discuss the method of calculations, we will describe briefly the tight-binding Hamil-

 © 1981 The American Physical Society

tonian used to study the electronic structure of Si (Ref. 8) and SiO_2.[9] In the case of the Si–Si bond we take all possible interactions between sp^3 orbitals in nearest-neighbor atoms; on the other hand, the Si–O bond is described by including only the σ interactions between the Si sp^3 orbitals and the $2s$ and $2p$ O orbitals. The Hamiltonian parameters are shown in Table I. The relative position of the energy of the Si sp^3 orbital (U_h) in Si with respect to its value in SiO_2 is fitted to optical-absorption data in the Si-SiO_2 interface.[10] The value of this parameter for SiO_x is linearly interpolated[11] between the extreme concentration values according to the number of oxygen atoms nearest neighbor of the Si atom we are dealing with.

To simulate the atomic structure of SiO_x we assume that the distribution of Si and O is such that: (i) We assume perfect tetrahedral coordination of the Si atoms irrespective of the kind of their nearest-neighbor atoms, since in all the different crystalline SiO_2 structures[12] and in amorphous SiO_x ($0 \leq x \leq 2$) films,[13] x-ray and electron diffraction measurements indicate that the tetrahedral coordination of the Si atoms is kept, indicating sp^3 hybridization. (ii) No oxygen bonds are allowed in the structure. (iii) The Si–O–Si bond angle is assumed fixed and we first take it to be $\theta = 144°$ as in α-quartz SiO_2 (Ref. 12) and the most probable value in amorphous SiO_2.[13] (iv) The continuous random network of atoms forms a Bethe lattice with no closed rings of bonds.

TABLE I. Hamiltonian parameters (in eV) for both the Si-Si and the Si-O interactions in the SiO_x alloy. The self-energies of the s and p orbitals at an Si atom depend on the number of oxygen atoms attached to it. This is due to the fact that we are dealing with orthogonal orbitals and to the charge transfer in the Si–O bond (Ref. 11). The values shown in the table for the Si–Si and Si–O bonds refer to an Si atom surrounded by four silicon atoms and by four oxygen atoms, respectively. In the other cases the values are linearly scaled.

Si–Si bond			
$\langle Si_s \vert H \vert Si_s \rangle =$	-1.8	$\langle Si_s \vert H \vert Si'_s \rangle =$	-1.7
$\langle Si_p \vert H \vert Si_p \rangle =$	6.2	$\langle Si_p \vert H \vert Si'_s \rangle =$	-2.25
		$\langle Si_p \vert H \vert Si'_p \rangle_\sigma =$	3.5
		$\langle Si_p \vert H \vert Si'_p \rangle_\pi =$	-1.0
Si–O bond			
$\langle Si_s \vert H \vert Si_s \rangle =$	1.7	$\langle Si_s \vert H \vert O_s \rangle =$	-3.9
$\langle Si_p \vert H \vert Si_p \rangle =$	8.1	$\langle Si_p \vert H \vert O_s \rangle =$	-6.06
$\langle O_s \vert H \vert O_s \rangle =$	-16.5	$\langle Si_s \vert H \vert O_p \rangle =$	-4.48
$\langle O_p \vert H \vert O_p \rangle =$	-1.3	$\langle Si_p \vert H \vert O_p \rangle_\sigma =$	-5.5

In order to calculate the electronic structure, we first use the Kittler and Falivov (KF) method[14,15] based on the cluster-Bethe-lattice approximation.[16] In this method the local configuration around the atom in which one is interested, is treated exactly and the rest of the system is simulated by an effective Beth lattice. In this Bethe lattice the SiO_x alloy is characterized by the bond probabilities and valence saturation. In this alloy, since there are no oxygen–oxygen bonds, we are restricted to the branch of the binary compound sequence[15] where Si is the majority species.

The calculation of the density of states for the above-described Hamiltonian involves dealing with four-by-four matrices. In particular one has to solve two different four-by-four transfer matrices ($\underline{T}_1$ and $\hat{\underline{T}}_1$) related to the direct Si–Si and to the oxygen-mediated Si–Si bonds, respectively. The equations that give these transfer matrices have the following form:

$$\underline{T}_1 = \left(\underline{W}^0 - \zeta_{\text{Si-Si}} \sum_{i=2}^{4} \underline{U}_i^+ \cdot \underline{M}_1 \cdot \hat{\underline{T}}_1 \cdot \underline{U}_i - \underline{Z}_{\text{Si-Si}} \sum_{i=2}^{4} \underline{U}_i^+ \cdot \underline{W}_1 \cdot \underline{T}_1 \cdot \underline{U}_i \right)^{-1} \cdot \underline{W}_1 \,, \tag{1a}$$

$$\hat{\underline{T}}_1 = \left(\underline{M}^0 - \zeta_{\text{Si-O}} \sum_{i=2}^{4} \underline{U}_i^+ \cdot \underline{M}_1 \cdot \hat{\underline{T}}_1 \cdot \underline{U}_i - Z_{\text{Si-O}} \sum_{i=2}^{4} \underline{U}_i^+ \cdot \underline{W}_1 \cdot \underline{T}_1 \cdot \underline{U}_i \right)^{-1} \cdot \underline{M}_1 \,. \tag{1b}$$

The subindex distinguishes between the four different sp^3 hybrid directions. The matrices $\underline{W}_i$ ($\underline{M}_i$) ($i = 1, 4$) refer to the direct (oxygen-mediated) interaction between nearest-neighbor silicon atoms, whereas $\underline{W}^0$ ($\underline{M}^0$) refers to the silicon self-energy when its parent is Si (oxygen). The matrices $\underline{U}_i$ are matrices corresponding to the tetrahedral symmetry operations. As in the original paper by Kittler and Falicov,[15] $Z_{\alpha\beta}$ ($\zeta_{\alpha\beta}$) is the probability that an α atom with a β parent has a like (unlike) descendant. Once the transfer matrices are solved numerically by an iterative procedure, the density of states is immediately obtained in the usual way.

The calculated densities of states for different concentrations and for a one-atom cluster are shown in Fig. 1. In this figure we notice the following points; Firstly, the p-bonding and p-nonbonding peaks characteristic of SiO_2 at -6 and -2 eV, respectively, are already present at $x \leq 1$. Secondly, the conduction-band edge has a smooth variation with concentration. Thirdly, the top of the valence band (at 3 eV at $x = 0$) has a striking behavior; its energy increases with the concentration and there is a p-bonding-like Si split-off band at the Si-gap energies. This behavior combined

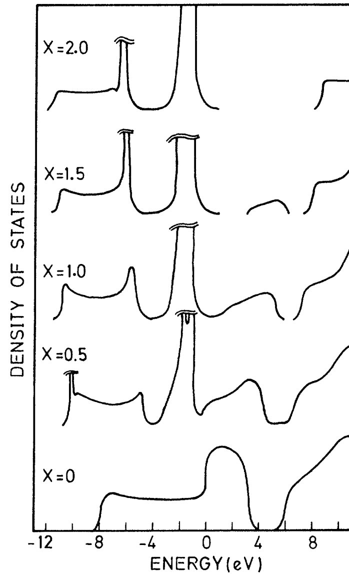

FIG. 1. Density of states of amorphous SiO_x calculated using the Kittler-Falicov method in the one-atom cluster approximation. A small (0.1 eV) imaginary contribution to the energy has been introduced for computational convenience.

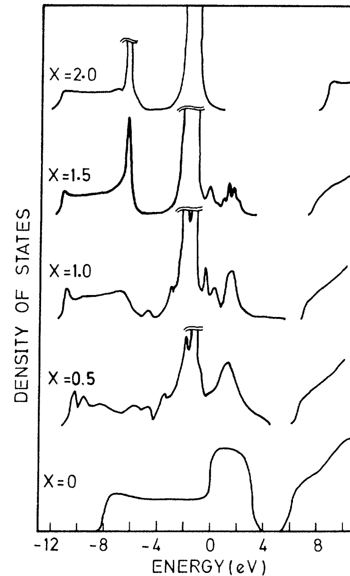

FIG. 2. Density of states of amorphous SiO_x calculated using the Kittler-Falicov method in the 17-atom cluster approximation. The distribution of oxygens in the cluster is assumed to be random. A small (0.1 eV) imaginary contribution to the energy has been introduced for computational convenience.

with the variation at the bottom of the conduction band makes the gap smaller as the oxygen concentration increases in open contradiction with optical-absorption experiments.[6] In the spirit of the cluster-Bethe-lattice method we increase the size of the central cluster of atoms to get a better description of the density of states. In Fig. 2 we show the densities of states calculated for a cluster which includes exactly the Si next-nearest-neighbor of the central atom; the oxygen atoms compatible with each concentration are randomly distributed in the cluster. For each concentration sufficient clusters were calculated to simulate randomness (the total weight of the clusters considered was 0.98). The results shown in Fig. 2 represent the average densities of states. As we notice immediately in this figure, the results are very similar to those corresponding to the one-atom cluster except for the split-off band which is essentially suppressed. This indicates that the effective medium in the Bethe lattice induces a spurious band at the Si-gap energies.

A simple way to understand the origin of this spurious band is by working with a simplified Hamiltonian like that described in the Appendix. In this Hamiltonian, the top of the Si valence band is represented by a twofold-degenerate δ-function which position in energy is given by

$$E = U_h + V - \Delta , \tag{2}$$

where U_h, V, and Δ are defined in the Appendix. In the KF approximation the interaction in the effective medium is taken to be pV where p is the probability that the nearest neighbor of an Si atom be also Si. It is clear that if $p < 1$ (as in the case of SiO_x with $x > 0$), Eq. (2) indicates that the Si p bonding peak merges into the gap. This is indeed what happens for our more realistic Hamiltonian (see Fig. 1) where the δ function of the simplified Hamiltonian is broadened into a band by the presence of the $pp\pi$ interaction.[8]

From the previous discussion we conclude that a mean-field approximation is not appropriate for discussing the SiO_x alloy because the top of the valence band is governed by the Si-Si interaction alone. On the other hand, the bottom of both the valence and conduction band are well described by the KF method since the corresponding states are a mixture of Si and O orbitals.

In order to overcome the inadequacy of mean-field approximation, one is faced with two possibilities; on the one hand, one could increase the size of the cluster and on the other hand, one could go beyond the mean-field approximation in the Bethe lattice, keeping the local cluster small enough. We have ruled out the first possibility for practical reasons since the computation time increases very rapidly with the size of the cluster. We then take the second approach. We deal with

exact Bethe lattices where the lattice sites are occupied by real atoms such that the interactions between them are not treated probabilistically. These Bethe lattices are formed by the most probable Si-(Si_y-O_{4-y}) unit in a random-bonding model[5,7] compatible with the concentration. In this way we can only treat the concentrations $x=0$, 0.5, 1.0, 1.5, and 2. The Bethe lattices for $x=0.5$, 1.0, and 1.5 are such that each Si atom is surrounded by one oxygen and three silicons, two silicons and two oxygens, and three oxygens and one silicon, respectively (see Fig. 3). To calculate the densities of states associated with these Bethe lattices we deal with four different transfer matrices for each concentration. Results of the calculated densities of states are also drawn in Fig. 3. As we can see, the behavior of the top of the valence band, in this approach and using the KF method (Fig. 1), is very different.

As shown in the Appendix, the presence of an oxygen atom forbids the propagation of the Si states near the top of the Si valence band. This effect means that, as far as the Si states near the gap are concerned, the Bethe lattice for $x=0.5$, 1.0, and 1.5 are like the threefold coordinated Si Bethe lattice, the twofold coordinated Si Bethe lattice, and a Bethe lattice decoupled into pairs of sp^3 Si hybrids, respectively. Our calculation shows that even for a realistic tight-binding Hamiltonian the position of the top of the valence band for SiO_x is essentially fixed in energy as long as there are infinite Si chains in the Bethe lattice (see the Appendix).

We have repeated the described cluster-Bethe-lattice calculation using these Bethe lattices as boundary conditions. Results of our calculation are shown in Fig. 4. The main features of the densities of states that we can notice are the following: (i) The bottom of the valence band changes abruptly from the pure Si value to the pure SiO_2 value from $x=0$ to $x=0.5$. (ii) The p-bonding peak at ~−7 eV, which is related to the presence of Si-O chains in the alloy, indeed appears for $x \geq 1$, since for $x=1$ the probability of the presence of these chains is nonzero. (iii) The p-nonbonding peak at ~−1.5 eV, which is related to the oxygen lone orbital, is present for $x>0$. (iv) The top of the valence band, indicated by an arrow, varies smoothly with concentrations changing abruptly to the SiO_2 position for $x \geq 1.5$. (v) The bottom of the conduction band varies smoothly with the concentration.

It should be noted that all the above-discussed features, with the exception of the behavior of the top of the valence band, are also reproduced by the calculation using the KF method. It is worthwhile indicating that when we refer to the presence of *infinite* Si or Si-O chains we mean *large enough* chains. As indicated in the Appendix, a chain of about ten Si atoms or an even-membered ring of Si–Si bonds already reproduces the top of the valence band corresponding to an infinite chain.

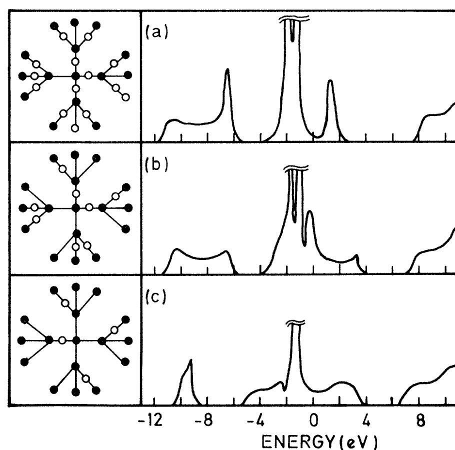

FIG. 3. Density of states corresponding to the exact Bethe lattices of SiO_x formed by the most probable Si(Si_y-O_{4-y}) units. (a) $SiO_{1.5}$, (b) SiO, and (c) $SiO_{0.5}$. A portion of the Bethe lattices is also drawn. A small (0.1 eV) imaginary contribution to the energy has been introduced for computational convenience.

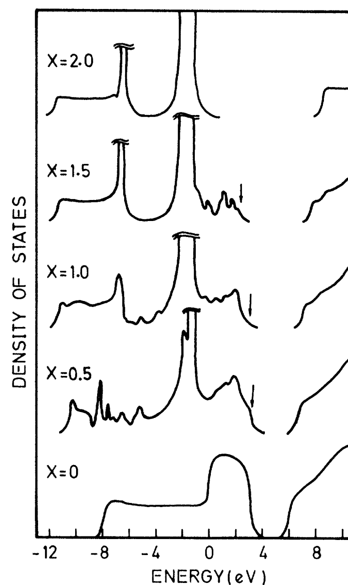

FIG. 4. Density of states of amorphous SiO_x in the 17-atom cluster-Bethe-lattice approximation. The clusters are embedded in the Bethe lattices of Fig. 3, compatible with each concentration. The arrows indicate the position of the highest valence-band energy level. A small (0.1 eV) imaginary contribution to the energy has been introduced for computational convenience.

This result emphasizes the importance of intermediate-range order; *the top of the valence band is governed by intermediate-range order*.

III. COMPARISON WITH EXPERIMENTS

In this section we compare the results of our calculation with different available experimental data. Optical-absorption experiments on SiO_x for the entire range of concentrations indicate a very nonlinear variation of the optical gap with concentration. The experimental results[6] are drawn in Fig. 5. We observe that the gap varies linearly between $x=0$ and $x\simeq 1.5$ where it changes abruptly to the SiO_2 value. Our calculated gap (see Fig. 4) is also indicated in Fig. 5. As we see, there is a reasonable agreement between theory and experiments. From the discussion of the previous section, we interpret the break in the variation of the gap with concentration at $x \simeq 1.4$ as being due to the breaking of Si chains due to the increase of oxygen in the alloy. The concentration at which the discontinuity takes place corresponds to the percolation[17] threshold in the Bethe lattice, i.e., at $x_c=1.33$. It should be noticed that this value of x_c is lower bound since the top of the valence band is governed by intermediate-range order (see the above discussion). The simple break of the infinite chains of Si is not enough to shift appreciably the position of the valence-band edge, since it remains essentially unchanged when finite Si chains about only ten atoms long are present in the alloy. Also it should be noticed that in a real alloy the presence of even-membered rings of bonds fixes the position of the top of the valence band (see the Appendix).

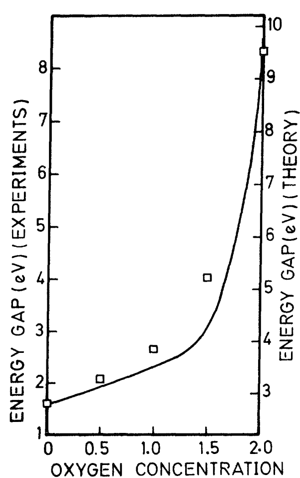

FIG. 5. Variation of the optical gap with concentration in the SiO_x alloy. The experimental data (Ref. 6) are indicated by a continuous curve and the calculated values are indicated by squares. The theoretical results are shifted for a better comparison with the experimental data.

The slope of the experimental optical-absorption curves[5,6] near threshold change from aburpt near $x=0$ and 2 to smooth near $x=1.5$. This behavior is consistent with our results since an abrupt slope indicates optical absorption due to delocalized states, whereas a smooth slope is related to optical absorption involving localized states. A comparison between Figs. 3 and 4 indicates that the states at the top of the valence band for $x=0$, 0.5, 1.0, and 2 are delocalized. On the other hand, the top of the valence band for $x=1.5$ is formed by localized states.

There are available ultraviolet photoemission data for $x=0$, 1.0, and 2.0. For $x=0$, the calculated density of states is in good agreement with experiments.[3,4] The experimental results and the calculated density of states for SiO_2 are drawn in Fig. 6. The main features of the experimental spectrum are well reproduced by our calculation, the main discrepancy being the width of the nonbonding band centered around −2 eV which is narrower and is shifted in the calculation with respect to the experiments. This behavior is due to the absence of the $pp\pi$ interaction in the Si–O bond in our Hamiltonian.

In Fig. 7(a) we present the UPS data[4] for an SiO film. A comparison of this figure with Fig. 6(a) reveals several differences between the SiO_2 and the SiO UPS spectra. First, the bottom of the valence band at ~−10.5 eV in SiO_2 is shifted upwards by ~1 eV in SiO. Second, the p-bonding peak is also shifted by ~0.5 eV and is weaker in SiO than in SiO_2. Third, there is a tendency in SiO to fill up the dip between the p-bonding and the p-nonbonding peaks. Fourth, the p-nonbonding peak at ~−2 eV is narrower in SiO than in SiO_2

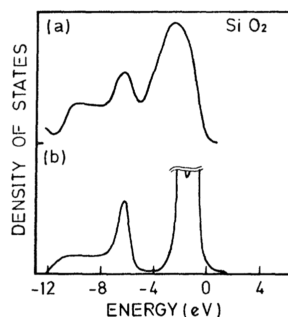

FIG. 6. (a) Experimental UPS data (Ref. 4) and (b) calculated valence-band density of states for SiO_2. The theoretical data have been convoluted with a Gaussian of 0.45 eV half-width at half maximum.

since there are fewer oxygen atoms. Fifth, in SiO there is a new band above the p-nonbonding peak. In Fig. 7(b) we present the broadened density of states for SiO (see Fig. 4 for $x=1.0$). There is an overall agreement between theory and experiments. The p-bonding peak at ~ -6.8 eV is weaker in SiO than in SiO_2 since there are fewer Si–O bonds in SiO than in SiO_2. There is, in our calculation, a tendency to fill up the dip between p-bonding and p-nonbonding peaks owing to the appearance of localized states associated with the disorder in the alloy. The band above the p-nonbonding peak is due to the presence of Si–Si bonds. It is important to notice that the calculated bonding band is shifted ~0.6 eV with respect to experiments.

So far we have assumed no bond-length and no bond-angle variation when alloying. In a recent work based on a chemical-shift analysis, Grunthaner *et al.*[2] have proposed that near the Si-SiO_2 interface the most probable Si–O–Si bond angle is 125°. This result is in addition to the fact that Hollinger[3] has found that the UPS spectra of SiO and of the Si-SiO_2 interface are very similar, indicating that the discrepancy between theory and experiment in Fig. 7 may be due to the fact that we have taken an inappropriate bond angle. We have repeated our calculation taking 125° for the Si–O–Si bond angle. The results are shown in Fig. 7(c). We now get a much better agreement with Hollinger's UPS data. There are two main effects due to the bond-angle variation. First, the bonding band is shifted to the right position and there is more tendency to fill the dip between the

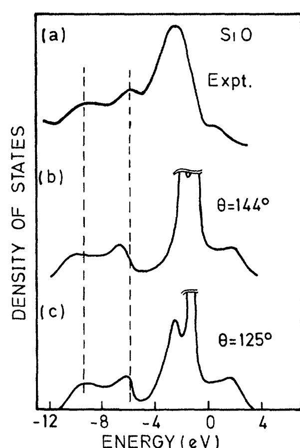

FIG. 7. (a) Experimental UPS data (Ref. 4) for SiO. (b) Calculated valence-band density of states (see Fig. 4) for SiO with an Si–O–Si bond angle of 144°. (c) The same calculation performed with an Si–O–Si bond angle of 125°. The theoretical data have been convoluted with a Gaussian of 0.45 eV half-width at half maximum.

bonding and nonbonding bands. It can be shown[18] that the variation of the position of the bonding band with the Si–O–Si bond angle goes like

$$E_{\text{bonding}} \sim T \sin\theta/2 \,, \qquad (3)$$

where T is defined in the Appendix. On the other hand, the nonbonding band behaves like

$$E_{\text{nonbonding}} \sim T \cos\theta/2 \,. \qquad (4)$$

This explains the two main effects of the bond angle variation.

It is generally accepted that the distribution of the silicon and oxygen atoms in SiO_x depends on the preparation of the sample. Each SiO_x composition is described by a set of distribution probabilities $P_y(x)$ for the five elemental tetrahedral units Si-(Si_y-O_{4-y}) ($y=1,4$).[7] In the random-bonding model, $P_y(x)$ represents the binomial distribution

$$P_y(x) = \frac{4!}{(4-y)!\,y!}\left(\frac{x}{2}\right)^{4-y}\left(1-\frac{x}{2}\right)^{y} . \qquad (5)$$

On the other hand, in the ideal-mixture model there is a tendency to form Si-Si_4 and Si-O_4 tedtrahedra. Then

$$[P_y(x)]_{y=0} = x/2 \qquad (6a)$$

and

$$[P_y(x)]_{y=4} = 1 - x/2 \,. \qquad (6b)$$

In our calculation we have assumed a distribution of Si and O atoms corresponding to the random-bonding model. We have also calculated densities of states for distributions of atoms other than the random one. We have not found very significant differences with respect to the above-reported results. This suggests that it is very difficult to infer the bonding statistics of an SiO_x system using UPS spectra. However, the percolation threshold is very sensitive to the bonding statistics. The critical concentration x_c for the random model is smaller than for the mixture model since, in this case, there is a higher probability of having long Si-Si chains in the system.

IV. CONCLUDING REMARKS

We have presented in this paper a realistic calculation of the electronic structure of amorphous SiO_x. The ingredients of our model are the following: (i) We have taken a realistic tight-binding Hamiltonian which describes properly the electronic structure of both Si and SiO_2. Once the Hamiltonian parameters for Si and SiO_2 are fixed, the only new parameter in the theory is the relative position of the Si sp^3 orbitals in Si and in SiO_2 which is fixed fitting optical-absorption data in Si-SiO_2. (ii) The Si and O atoms are distributed

in a Bethe lattice such that there are no O–O bonds. The calculation of the densities of states are made using the cluster-Bethe lattice method. (iii) Given the inadequacy of previous mean-field theories to deal with SiO_x, we have used a boundary conditions of finite clusters exact Bethe lattices. In these Bethe lattices, the distribution of the Si and O atoms is fixed for each concentration.

Results of our calculations allow us to conclude: (a) There is no evidence for deviations of random distribution in the SiO_x samples corresponding to the experiment with which we have compared. The distribution of Si and O atoms is random with no O–O bonds. (b) The bond angle Si–O–Si in SiO is close to 125° instead of being 144° as in α-quartz. (c) The behavior of the SiO_x gap is essentially due to the fact that chains and even-membered rings of Si atoms in the alloy fix the position of the valence-band edge. (d) The electronic structure of a-SiO_x is governed by intermediate-range order. Long-range order is lost and short-range order alone cannot properly describe a-SiO_x.

ACKNOWLEDGMENT

This work was supported in part by the U.S.–Spain Friendship and Cooperative Treaty, Complementary Agreement No. 3.

APPENDIX

In this Appendix we study, using a simplified Hamiltonian, the behavior of the top of the valence band of SiO_x. Let us take a simple tight-binding Hamiltonian for SiO_2 including the following interactions:

$$\langle h,i|H|h,i\rangle=\Delta\ , \tag{A1a}$$

$$\langle h,i|H|h,i\rangle=U_h\ , \tag{A1b}$$

$$\langle s,\alpha|H|s,\alpha\rangle=U_s\ , \tag{A1c}$$

$$\langle p,\alpha|H|p,\alpha\rangle=U_p\ , \tag{A1d}$$

$$\langle h,i|H|s,\alpha\rangle=t\ , \tag{A1e}$$

$$\langle h,i|H|p,\alpha\rangle=T\ , \tag{A1f}$$

where $|h,i\rangle$ stands for the sp^3 hybrid of the silicon atom, i pointing to the nearest-neighbor oxygen atom labeled α. $|s,\alpha\rangle$ represents the $2s$ orbital of the oxygen atom α and $|p,\alpha\rangle$ is the $2p$ orbital of this oxygen atom oriented in the Si–O bond direction. The SiO_2 lattice can be reduced to an effective Si lattice[19,20] described by a Weaire-Thorpe Hamiltonian[21] such that the effective Si-Si interactions are now energy dependent:

$$\langle h,i|H'|h',i\rangle=\Delta \tag{A2a}$$

$$\langle h,i|H'|h,i\rangle=U_h+\frac{T^2}{E-U_p}+\frac{t^2}{E-U_s}=U_h^{\mathrm{eff}}(E)\ , \tag{A2b}$$

$$\langle h,i|H'|h,i'\rangle=\frac{T^2\cos\theta}{E-U_p}+\frac{t^2}{E-U_s}=V^{\mathrm{eff}}(E)\ , \tag{A2c}$$

where θ is the Si–O–Si bond angle of the original SiO_2 lattice.

This scheme can be easily extended to an SiO_x system. In this case, the hybrids of an Si atom can have two different self-energies: U_h^{eff} if the hybrid is pointing towards an oxygen atom or if U_h is pointing towards a silicon atom. The interaction between hybrids of nearest-neighbor Si atoms would be V^{eff} is there is an oxygen atom between them, and otherwise V.

For any reasonable set of Hamiltonian parameters, $U_h^{\mathrm{eff}}-U_h$ is one order of magnitude greater than Δ in the Si-gap energy region. This shows that in this energy region two hybrids at the same silicon atom, such that one points towards an oxygen atom and the other towards a silicon atom, are essentially noninteracting. Therefore, the SiO_x system can be visualized, for energies in the Si-gap region, as being formed by two independent sublattices: one sublattice includes all hybrids of the Si–O–Si bonds (SiO_2-like sublattice); the other sublattice includes all the hybrids of the Si–Si bonds (Si-like sublattice). These two sublattices can be studied separately as Si lattices so that in the SiO_2-like sublattice the interactions are effective interactions (A2).

The top of the valence band of the SiO_2-like sublattice is always at the lone-orbital energy, i.e., at $E_v^{SiO_2}=U_p$. On the other hand, if the Si-like sublattice were perfectly tetrahedrally coordinated, its valence-band edge would be at[21]

$$E_v^{Si}=U_h+V-\Delta\ , \tag{A3}$$

this energy being well above $E_v^{SiO_2}$. One can easily prove that the spectral bounds of the Si-like sublattice at (A3) and at

$$E_c^{Si}=U_h-V+3\Delta \tag{A4}$$

are in the energy region where the decoupling is almost complete. This shows that if there are no defects in the SiO_x system the Si band gap is a forbidden region.

We have to find under which conditions the spectral bounds are saturated. We will show that the valence-band edge (A3) is kept fixed as long as there are infinite Si-Si chains or even-membered rings of Si–Si bonds in the SiO_x system. In other words, when the Si-like sublattice forms a contin-

uous network.

Let the eigenfunctions of the Si-like sublattice be written as

$$|\psi(E)\rangle = \sum_{ih} C_h^i(E)\,|h,i\rangle\,, \quad (A5)$$

where i indicates the Si atoms and h the sp^3 orbitals. The subindex h runs from 1 to $n(i)$, $n(i)$ representing the coordination of the atom i in the Si-like sublattice. We can now write the eigenvalue equation

$$H\,|\psi(E)\rangle = E\,|\psi(E)\rangle\,. \quad (A6)$$

For any nearest-neighbor pair of Si atoms labeled i and i' we can write

$$(E + \Delta - U_h)C_h^i(E) = \Delta \sum_{h'}^{n(i)} C_{h'}^i(E) + V C_h^{i'}(E)\,. \quad (A7)$$

A solution of (A6) is

$$\sum_{h'}^{n(i)} C_{h'}^i = 0 \quad \text{for all } i\,, \quad (A8a)$$

$$C_h^i(E) = C_h^{i'}(E) \quad (A8b)$$

if there are infinite coupled equations (A7) (i.e., if there are infinite chains of Si–Si bonds) or if the atoms form an even-membered closed ring.

The solution (A8) gives the eigenvalue $E = U_h + V - \Delta$ as in (A3). Then the spectral bound is saturated. A question we ask ourselves is how long the Si chains have to be, in order to be close to the spectral bound. For an Si one-dimensional chain and a given set of parameters we get 2.0, 2.9, 3.1, and 3.2 eV for the position of the valence band for two, six, ten, and infinite bonds, respectively. From the above discussion we conclude that the top of the valence band of an SiO_x system is close to the pure Si value as long as there are sufficiently long chains of Si bonds.

Finally we would like to remark that the decoupling approximation is also valid for a more realistic tight-binding Hamiltonian as that described in Sec. II. The δ function of E_v becomes a band centered at E_v (Ref. 8) with a width depending on the coordination of the Si-like sublattice.

[1] *The Physics of SiO_2 and its Interfaces*, edited by S. T. Pantelides (Pergamon, New York, 1978), and references therein.
[2] F. J. Grunthaner, P. J. Grunthaner, R. P. Vasquez, B. F. Lewis, and J. Maserjian, Phys. Rev. Lett. 43, 1683 (1979).
[3] G. Hollinger, These de Doctoral d'Etat, Université Claude Bernard, Lyon, 1979 (unpublished).
[4] G. Hollinger, Y. Jugnet, and Tran Minh Duc, Solid State Commun. 22, 277 (1977).
[5] H. R. Philip, J. Phys. Chem. Solids 32, 1935 (1971).
[6] E. Holzenkämpfer, F. W. Richter, J. Stuk, and U. Voget-Grote, J. Non-Cryst. Solids 32, 327 (1979).
[7] K. Hübner, J. Non-Cryst. Solids 36, 1011 (1980).
[8] V. T. Rajan and F. Yndurâin, Solid State Commun. 20, 309 (1976).
[9] R. B. Laughlin, J. D. Joannopoulos, and D. J. Chadi, Phys. Rev. B 20, 5228 (1979).
[10] T. H. Distefano, J. Vac. Sci. Technol. 13, 856 (1976).
[11] R. B. Laughlin, J. D. Joannopoulos, and D. J. Chadi, Phys. Rev. B 21, 5733 (1980).
[12] R. W. G. Wyckoff, *Crystal Structures* (Interscience, New York, 1965).
[13] C. F. George and P. D'Antonio, J. Non-Cryst. Solids 34, 323 (1979).
[14] L. M. Falicov and F. Yndurâin, Phys. Rev. B 12, 5664 (1975).
[15] R. Kittler and L. M. Falicov, J. Phys. C 9, 4259 (1976).
[16] J. D. Joannopoulos and F. Yndurâin, Phys. Rev. B 10, 5164 (1974).
[17] V. K. Shante and S. Kirkpatrick, Adv. Phys. 20, 325 (1971).
[18] E. Martinez and F. Yndurâin, Phys. Rev. B 21, 3589 (1980).
[19] F. Yndurâin, Solid State Commun. 27, 75 (1978).
[20] M. Bensoussan and M. Lannoo, J. Phys. (Paris) 40, 749 (1979).
[21] M. F. Thorpe and D. Weaire, Phys. Rev. B 4, 3518 (1971).